Nickel based superalloys: Micromechanics near the yield point

Jonas von Kobylinski[a], Christian Krempaszky[a], Ewald Werner[a] & Robert Lawitzki[b]

[a] Lehrstuhl für Werkstoffkunde und Werkstoffmechanik, TUM

[b] Institut für Materialwissenschaft - Lehrstuhl für Materialphysik Universität Stuttgart

Contact Information:

Lehrstuhl für Werkstoffkunde und Werkstoffmechanik
Technische Universität München
Boltzmannstraße 15
85748 Garching b. München
Phone: +49 (089) 289 15311
Email: woste@wkm.mw.tum.de

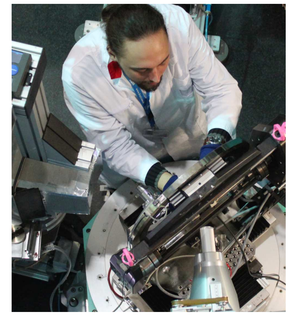

1 Introduction

Nickel based superalloys are known for retaining a high yield stress at elevated temperatures, a feature that is typically related to the presence of coherent, ordered precipitates. In related materials, segregation pinning by and diffusion of γ- (or matrix-) stabilizing elements to planar defects (e.g. those within superdislocations) within γ'-precipitates involve strain softening and belong to the important mechanisms governing creep and dynamic strain aging at elevated and high temperatures. Present study focuses on the phenomena of strain softening in Nickel based superalloys and, associatedly, on strain localization. Further, explanations for observed differences between different microstructures in their type-II residual stress evolutions during uniaxial tensile loading are required.

Figure 1: Photography taken after a part of Haynes 282 showed an unexpected response to hot forging.

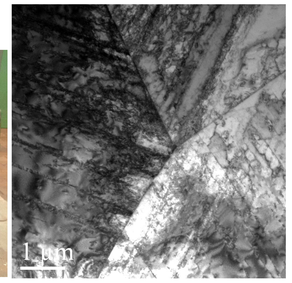

Figure 2: Post-mortem TEM-analysis of Haynes 282. Plastic flow takes the shape of slip band (indicating localized shear) in this material.

2 Finite element modeling

- Geometry: for the initial state, a cubic geometry was used
- Boundary conditions: periodic boundary conditions, stepwise increases to the length along z-direction in order to reproduce uniaxial loading boundary conditions
- Tesselation: 500 standard Voronoï tesselated grains
- Meshing: an average of 1000 (initially) cube- shaped elements (C3D8) were used per grain
- Constitutive model: phenomenological crystal plasticity

Phenomenological crystal plasticity is a commonly employed constitutive model. It was realized via the DAMASK implementation into the Abaqus FEM software. The used constitutive equations for plastic shear in each glide system α are:

$$\tau^{\alpha} = \mathbf{S} : \left(\mathbf{m}^{\alpha} \otimes \mathbf{n}^{\alpha}\right)$$
$$\dot{\gamma}^{\alpha} = \dot{\gamma}_0 \mid \frac{\tau^{\alpha}}{\tau_c^{\alpha}} \mid^{m} \operatorname{sgn}\left(\tau^{\alpha}\right)$$
$$\dot{\tau}_c^{\alpha} = \mathbf{q}_{\alpha\beta} \mathrm{h}_0 \left(1 - \frac{\tau_c^{\beta}}{\tau_{\mathrm{s}}}\right)^{a} \cdot \mid \dot{\gamma}^{\beta} \mid$$

Here, $\mathbf{m}^{\alpha}$ and $\mathbf{n}^{\alpha}$ are the slip direction and the plane normal of the respective slip system, τ^{α} is the resolved shear stress (analogous to Schmid's law), $\dot{\gamma}^{\alpha}$ is the shear rate, τ_c^{α} is the critical resolved shear stress, and τ_{s} describes the saturation of hardening. Einstein's summation convention is used in the last formula.

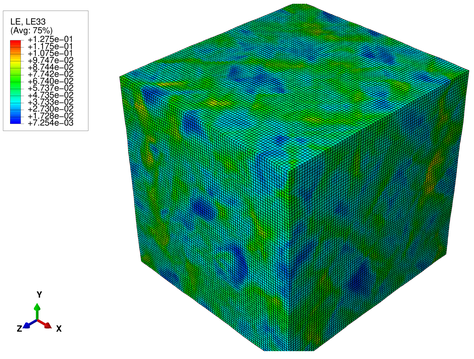

Figure 3: Visualization of the strain components along tensile direction (z) within a plastically deformed Representative Volume Element (RVE) with 500 randomly oriented grains simulating Haynes 282.

3 Experimental

Present work investigates the micromechanical behaviour of polycrystalline Haynes 282 and Inconel 718. In-situ neutron diffraction during tensile testing selectively studies certain lattice spacings, thereby yielding elastic strain components of crystallites which are aligned with a representative of a certain family of cryst. directions along the respective measurement directions within the typically large gauge volumes. Each sample was deformed step-wise and measured along various directions for each deformation step for multiple reflections.

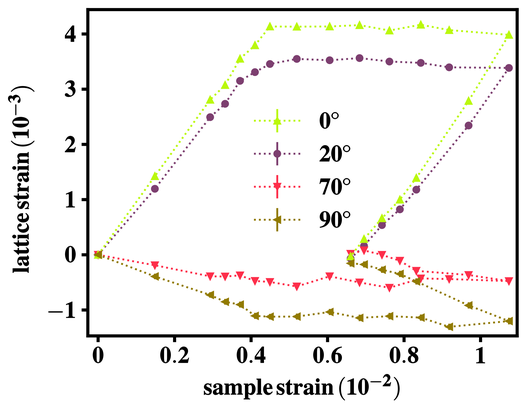

Figure 4: Lattice strain of the (220) reflection over sample strain measured along four different directions. The included dotted lines are guides to the eye. The included standard error bars are typically smaller than the symbols. The specimen which had its heat treatment intermitted with plastic deformation displayed no pronounced non-monotony during tensile testing.

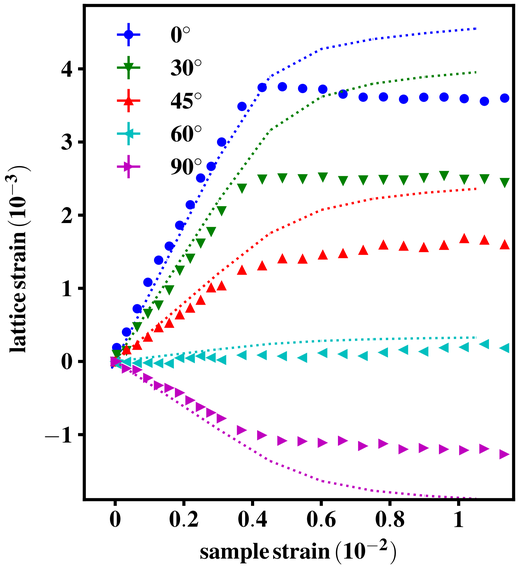

Figure 5: Lattice strain of the (220) reflection over sample strain measured along five different directions. The included standard error bars are typically smaller than the symbols. The included dotted lines represent output from a crystal plasticity based model and deviate strongly from experimental data. The deviation is accompanied by non-monotonous lattice strain evolutions along tensile direction (0°, blue data).

4 Conclusions

- Commonly employed formulations of phenomenological crystal plasticity, despite describing texture- and some lattice strain evolutions well (not shown here), predict neither the experimentally observed non-monotonous lattice strain evolutions nor slip band formations.
- Associated phenomena with softening mechanisms are dynamic strain ageing, strain localization (often in the shape of slip bands), and an initially low (macroscopic) work hardening rate.
- Diffusion of γ'-promoting solute elements with diffusion paths on the order of the size of typical precipitates (about 25 nm) does not promote non-monotonous lattice strain evolution, despite the presence of slipbands (realized via previously deformed and heat treated specimens).
- A micromechanical description of present materials requires a model depicting softening and strain localization. Our studies give micromechanical inputs into this model's behaviour at elevated temperatures and during repeated loading and unloading.

References

[1] Jonas von Kobylinski, Robert Lawitzki, Michael Hofmann, Christian Krempaszky, and Ewald Werner. Micromechanical behaviour of Ni-based superalloys close to the yield point: a comparative study between neutron diffraction on different polycrystalline microstructures and crystal plasticity finite element modelling. *Continuum Mechanics and Thermodynamics*, 31(3):691–702, 2019.

5 Acknowledgements

This research was funded by DFG grant number 280883331.